ACS APPLIED NANO MATERIALS

www.acsanm.org Article

Noncovalently Functionalized Halloysite Nanotubes for Use in Reinforced Polymer Composites

Danae L. Francisco,* Lucilene B. Paiva, Wagner Aldeia, Ademar B. Lugão, and Esperidiana A. B. Moura

Cite This: *ACS Appl. Nano Mater.* 2020, 3, 11510−11516 Read Online

ACCESS | Metrics & More | Article Recommendations | Supporting Information

ABSTRACT: The inorganic halloysite nanotube (HNT) is a promising type of naturally occurring fillers with many important uses in different fields. An HNT has a relatively low content of hydroxyl groups on its surface, which makes it relatively hydrophobic, although this is not always sufficient to guarantee good interfacial adhesion in composite systems. Further surface treatment is required to improve the compatibility of HNTs with polymer matrixes, maximizing interfacial interactions. The aim of the present work was to study a noncovalent functionalization of halloysite with 2,2′-(1,2-ethenediyldi-4,1-phenylene) bisbenzoxazole (EPB), based on electron transfer, for further use of EPB as a coupling agent in polymer/HNT compatibility. A set of characterization techniques were performed to evaluate the chemical and physical properties and evidence the functionalization. The results revealed the surface modification of halloysite upon functionalization. Emphasis was for powder wettability by tensiometry based on Washburn because no studies about halloysite powders using this technique could be found in the literature. The results demonstrate a reduction in the total surface energy of the system, usually accompanied by a reduction in the polar component upon HNT modification.

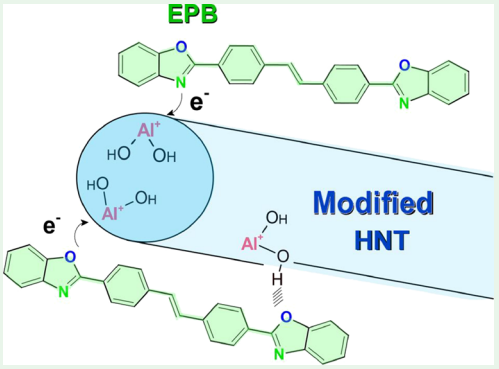

KEYWORDS: *halloysite, functionalization, surface modification, surface energy, tensiometry*

1. INTRODUCTION

The name "halloysite" originated from Omalius d'Halloy, who was responsible for finding the mineral in Angleur, Lieége, Belgium.[1] The halloysite nanotube (HNT) is a natural multiple-walled inorganic nanotube (1D), with geometry similar to that of carbon nanotubes.[2] The HNT chemical formula is $Al_2Si_2O_5(OH)4.nH_2O$, where n can vary from 0 to 2, representing dehydrated (interlayer space of 7 Å) and hydrated (interlayer space of 10 Å) halloysite polymorphs, respectively.[1,3,4]

Halloysite is a dioctahedral 1:1 clay mineral that belongs to the kaolin group.[3] The unit layer of this group is composed of one SiO_4 tetrahedral sheet (where one SiO tetrahedron is linked to three adjacent ones by sharing three basal-oxygen atoms forming an infinite 2D sheet) and one $AlO_2(OH)_4$ octahedral sheet (where AlO octahedrons are connected by sharing edge-forming sheets with hexagonal or pseudohexagonal symmetry). In the case of halloysite, the adjacent unit layers are separated by one monolayer of water molecules. The dominant tubular morphology of HNTs results from the wrapping of its layers under favorable geological conditions.[3] Most of the aluminol (Al−OH) groups are located in the inner (internal lumen and interlayer) part of the halloysite, while on the outer surface, the siloxane group (Si−O−Si) has a few silanols/aluminols on the edges of the sheets, However, some Al−OH and Si−OH groups are also exposed in halloysite surface defects.[3] The relatively small amount of hydroxyl groups (−OH) on the halloysite surface makes it relatively hydrophobic when compared with other clays and nanosilica.

HNT characteristics, such as tubular microstructure, reduced size (length between 50 nm and 5 μm, inner diameter between 5 and 100 nm, and outer diameter between 20 and 200 nm),[1,3,5,7] high aspect ratio (10−50), and high mechanical stiffness (elastic modulus 130−140 GPa), justify the increase in interest for its application, especially to produce polymer-based nanocomposites.[1,8]

Expressive research on halloysite began in the 1940s, and in recent years, halloysite has gained great attention as shown in Figure 1. Sometimes, its natural hydrophobicity (when compared with other clays) is not sufficient for interfacial adhesion in the composites; thus, HNT surface modification is necessary before its incorporation into polymers, to maximize its interfacial compatibility.[1,3,9]

HNTs tend to adsorb organics on its surface due to the electrostatic, hydrogen bonding, and electron transferring

Received: September 25, 2020
Accepted: October 13, 2020
Published: October 29, 2020

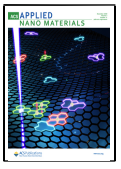

https://dx.doi.org/10.1021/acsanm.0c02600
ACS Appl. Nano Mater. 2020, 3, 11510−11516

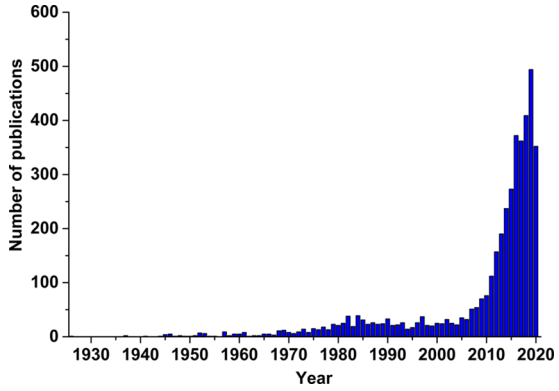

Figure 1. Publications about halloysite according to the Scopus database, 2020 (strategy "halloysite" in documents; search—articles' title, abstract, and keywords).

interactions.[3] The halloysite functionalization can be divided into two main groups: covalent functionalization and noncovalent functionalization.[1]

Several types of chemical compounds are employed to promote the surface modification of halloysite, such as γ-aminopropyltriethoxysilane or 3-aminopropyltriethoxysilane (APTES),[10−16] *N*-2-aminoethyl-3-aminopropyltrimethoxysilane (AEAPTMS),[10] (3-mercaptopropyl)trimethoxysilane (MPTMS),[10] (3-bromopropyl)-trimethoxysilane (BrTMS),[10] vinyltrimethoxysilane (VTMS),[10,17] phenyltriethoxysilane (PhTES),[10] glycidyl methacrylate (GMA),[18] octylphophonic acid (OPA),[19] γ-methacryloxypropyltrimethoxysilane (MAPTS),[20,21] γ-glycidoxypropyltrimethoxy (GPS),[22] 2,2′-(1,2-ethenediyldi-4,1-phenylene) bisbenzoxazole (EPB),[23] 2,5-bis(2-benzoxazolyl) thiophene (BBT),[24] phenylphosphonic acid (PPA),[25] alkyltrimethylammonium bromides,[6] sodium dodecanoate, and sodium dodecylsulfate.[26] In some of these studies, the modified HNT is incorporated in a polymeric matrix, ethylene propylene diene monomer (EPDM),[21] poly(vinylidene difluoride) (PVDF),[13] epoxy,[22] unsaturated polyester (UPE),[17] polypropylene (PP),[23,24] polyamide 6 (PA6),[14,20] polyamide-11(PA11)/ styrene-ethylene-butylene-styrene grafted maleic anhydride(SEBS-g-MA) blends,[15] and poly (lactic acid) (PLA).[16] A series of characterization techniques have been used to evidence the functionalization of HNTs, such as transmission electron microscopy (TEM), scanning electron microscopy (SEM), atomic force microscopy (AFM), energy-dispersive X-ray spectroscopy (EDS), Brunauer−Emmett−Teller (BET) method, X-ray diffraction (XRD), elemental analysis (EA), X-ray photoelectron spectroscopy (XPS), thermogravimetric analysis (TG), attenuated total reflectance−Fourier transform infrared (ATR-FTIR) spectroscopy, ζ potential, pyrolysis−gas chromatography/mass spectrometry (Py-GC/MS), and solid-state nuclear magnetic resonance (NMR).

Wettability is an important tool for measuring the powder surface property, which affects processes like dispersion, granulation, consolidation, dissolution, etc.[27] Some methods are used for this purpose, such as the sessile drop goniometric method (Heertjes and Kossen),[28] the plug method (Bartell and Whitney),[29] and the capillary penetration method (Washburn).[30] The goniometric method is based on image detection of a sessile drop. The method requires trained personnel for data analysis, and in case of hydrophilic powders, the liquid drop immediately penetrates into the powder surface, which does not guarantee a satisfactory image and reproducible data. In contrast, the Washburn method is a standard technique for powders and porous materials, based on the capillary rise of the liquid in a tube containing the powder and can be an interesting alternative to evaluate surface energy of the powder as well as its dispersive (apolar) and polar component.[27]

No studies of powder wettability using the modified Washburn method to characterize halloysite powders were found in the literature. Therefore, more investigations are needed to expedite the preparation of efficient HNT nanocomposites. Although the present study was based on the study by Liu et al. (2008), that is, the same type of functionalization was applied, the authors only characterized the functionalized HNT by BET and FTIR techniques. In this work a deep understanding of the possible interaction mechanisms between HNTs and EPB is presented. In addition to BET and FTIR, other techniques were applied to provide a complete characterization of physical and chemical modifications upon HNT functionalization. These characterizations include tensiometry to compare powder surface energy of pristine and modified HNTs, dynamic light scattering (DLS), zeta potential, thermogravimetry, and SEM. The HNT functionalization was aimed at its future incorporation, for a more compatible filler, in an engineering polymeric matrix (such as polyamide).

2. MATERIALS AND METHODS

2.1. Materials. Halloysite—empirical formula $Al_2Si_2O_5(OH)_4{\cdot}2H_2O$, molecular weight 294.19 g/mol (unitary cell of HNTs), density of 2.53 g/cm^3, diameter 30−70 nm, and length 1−3 μm (information provided by the manufacturer; CAS number 1332-58-7)—was purchased from Sigma-Aldrich. EPB—empirical formula $C_{28}H_{18}N_2O_2$ and molecular weight 414.45 g/mol (information provided by the manufacturer; CAS number 1533-45-5)—was also purchased from Sigma-Aldrich.

2.2. Functionalization of HNT. Pristine halloysite (100 wt % of the HNT) was modified with different percentages of EPB, such as 0.2 wt % (99.8HE), 5 wt % (95HE), and 10 wt % (90HE). The HNT was dried in a vacuum oven for 24 h at 80 °C before functionalization. The methodology of functionalization, based on Liu et al. (2008),[23] consisted of a direct mixture of halloysite and EPB powder. Both components in their respective proportions were added in an agate mortar and mixed vigorously with a pestle for 5 min.

2.3. Characterization Techniques. A set of characterization techniques was used to evaluate the surface modification of the halloysite with EPB.

Zeta potential and particle size by DLS were determined using NanoPlus-3 equipment from Micromeritics (Particulate Systems), and the samples (10 mg) were dispersed in deionized water (30 mL, pH ≈ 7) and sonified.

The thermal stability was evaluated using the thermogravimetric analysis (TG) technique utilizing the Mettler Toledo TGA/DSC1 STARe System. A duplicate of each sample (approximately 15 mg) was submitted to a heating program in a range of 25 to 1000 °C, with a constant heating rate of 10 °C/min, in a synthetic air atmosphere under 50 mL/min flow using an open alumina crucible.

The BET surface area was investigated using the nitrogen adsorption method utilizing Micromeritics Gemini V equipment. The samples were first degassed at a temperature of 80 °C until the pressure achieved 10 mmHg. The specific surface area was calculated by applying the BET method to the relative pressure (P/P_0) range of the isotherms between 0.06 and 0.2, taking a value of 0.162 nm^2 for the cross-section of the adsorbed nitrogen molecules at 77 K. Particle size of samples was also calculated using the BET surface area according to eq 1.[31,32]

https://dx.doi.org/10.1021/acsanm.0c02600
ACS Appl. Nano Mater. 2020, 3, 11510−11516

$$\text{BET particle size (nm)} = \frac{6000}{\text{BET surface area} \times \rho} \quad (1)$$

where 6000 is the shape factor for spherical particles (to be comparable with DLS analysis) and ρ = density (g/cm^3), for HNT = 2.5 g/cm^3 and for EPB = 1.4 g/cm^3.

The hydrophobicity experiment was performed according to Guo et al. (2009).[20] About 0.2 g of each sample was weighed and added to a separate test tube. First, 10 mL of toluene was added followed by bath sonication for 10 min, then deionized water was added, and again, sonication for 10 min was applied. Finally, the samples were kept for 24 h at rest to observe retention in the solvent.

The surface energy of samples was determined using a DCAP 11 DataPhysics tensiometer with a powder accessory kit (PUR 11). The modified Washburn equation (eq 2) was used to calculate the contact angle of each sample in three solvents (water, ethanol, and ethylene glycol) with different characteristics (Table 1), in addition to the *n*-hexane that was used to perform the calibration curve and determine constant C for each sample. To determine the surface energy of samples and its components (dispersive and polar), the Owens–Wendt–Kaelble model was applied in the equipment software, and the previously determined contact angle was considered.

Table 1. Total Surface Tension, Dispersive, and Polar Components of the Solvents

	surface tension (SFT)		
solvent	total (mN/m)	dispersive (mN/m)	polar (mN/m)
n-hexane	18	18	0
ethanol	24	19	4
ethylene glycol	48	29	19
water	72	20	52

$$W^2 = c\frac{\Upsilon_l \cos\theta \rho^2}{2\eta} t \quad (2)$$

where w = weight, ρ = liquid density, Υ_l = surface tension of the liquid, θ = advancing contact angle, η = liquid viscosity, and c = constant experimentally determined for each type of packing powder. The measurement must be done with the completely wetting liquid such as *n*-hexane, where the contact angle can be assumed as 0° (cos 0 = 1).

ATR-FTIR spectroscopy was performed to identify bands of the groups present in the chemical structure of pristine and functionalized halloysite. The assays were performed on a Thermo spectrometer, model Nicolet 8700/6700. A minimum of 64 scans was signal-averaged with a resolution of 4 cm^{-1} in a wavenumber range of 400–4000 cm^{-1}.

The high-resolution SEM was performed using FEI Quanta 3D model equipment with a field-emission gun source. The images were acquired using the equipment operating at 20 kV acceleration under high-vacuum conditions. The chemical characterization of some microstructural regions was made by dispersive energy spectroscopy coupled to the SEM. The samples were deposited to the sample holder with the aid of a carbon tape and covered with a thin Au/Pd film by sputtering to avoid surface charge.

3. RESULTS AND DISCUSSION

3.1. Zeta Potential and Particle Size. The diffusion coefficient and hydrodynamic diameter in water for pristine HNTs and modified HNTs were measured by DLS, and zeta potential was determined to evaluate the stability and surface charge modification, as shown in Table 2.

The DLS is typically interpreted in terms of sphere morphology particles, but the HNT has a tubular morphology, so DLS results in this case do not clearly correspond to a single dimension (length or diameter) but rather to a combined value. The polydispersity index of all samples was around 0.2. Pristine HNTs presented a hydrodynamic diameter average value of 330 nm in water, a value within the range reported in the literature.[1,4,8] HNTs showed a zeta potential of −15.8 mV, near the value observed by Pan et al. (2017) at a pH around 7 (in deionized water).[33] This negative charge was mainly due to the influence of silica present on its external surface with a small contribution from the positive alumina inside the inner surface.[4,34]

Table 2. Diffusion Coefficient, Hydrodynamic Diameter Average, Polydispersity Index, and ζ Potential for HNTs and Modified HNTs

sample	diffusion coefficient × 10^{-12} (m^2/s)	hydrodynamic diameter average (nm)	polydispersity index	ζ potential (mV)
HNT	1.5	330 ± 10	0.20	−15.8 ± 1.3
99.8HE	1.6	308 ± 2	0.21	−24.0 ± 0.4
95HE	1.2	409 ± 7	0.22	−24.2 ± 0.9
90HE	1.2	410 ± 47	0.24	−24.8 ± 0.6

Table 3. BET Specific Surface, C Constant, and Calculated Particle Size for HNTs and Modified HNTs

	BET		
sample	specific surface area (m^2/g)	C value	calculated particle size (nm)
HNT	54	155	283
99.8HE	44	107	342
95HE	41	101	362
90HE	38	95	380

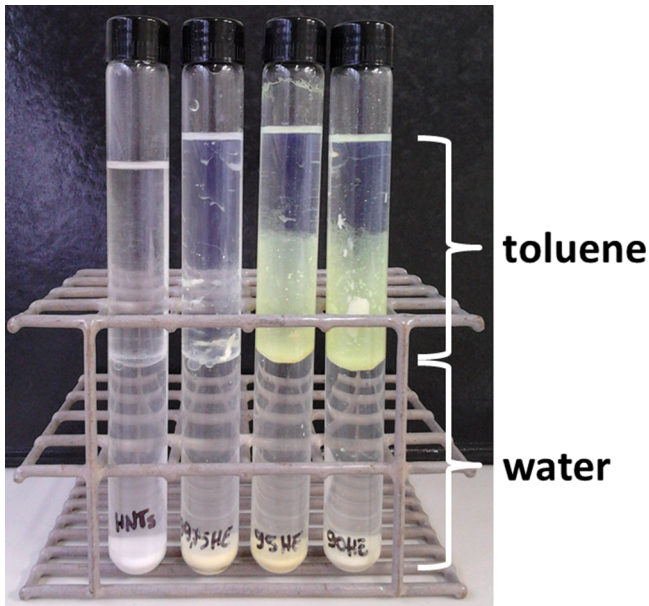

Figure 2. Water/toluene hydrophobicity experiment for the HNT and HNT modified with EPB (99.8, 95, and 90HE, respectively).

The decrease in the diffusion coefficient reflected the increased hydrodynamic diameter for the functionalized tubes. A significant increase was also observed in zeta-potential modulus after HNT modification. The interface between the halloysite and EPB may involve multiple mechanisms, such as Lewis acid–base interaction, van der Waals forces, and electron transfer, which could explain these results.[35] The inner and edge surface of HNTs, sometimes even its surface

https://dx.doi.org/10.1021/acsanm.0c02600
ACS Appl. Nano Mater. 2020, 3, 11510–11516

Table 4. Tensiometry Results of HNTs and HNTs Modified with EPB

	contact angle (°)						
sample	water	ethanol	ethylene glycol	surface energy (mN/m)	dispersive component (mN/m)	polar component (mN/m)	R^2
HNT	85	73	60	29	1.7	28	0.9
99.8HE	86	74	[a]	[a]	[a]	[a]	[a]
95HE	87	71	77	21	2.4	18	1.0
90HE	89	78	84	21	1.6	19	1.0

[a]The samples of 99.8HE present curves with different angular coefficients when ethylene glycol was used, which does not guarantee certainty in the contact angles of 99.8HE with this solvent.

Table 5. Thermogravimetric Weight Loss in Different Temperature Ranges for Pure and Modified HNTs and the Amount of EPB Adsorbed

			250–650 (°C)	
sample	25–100 (°C) wt (%)	100–250 (°C) wt (%)	wt (%)	EPB wt (%)
HNT	2.1	3.6	16.3	-
99.8HE	2.0	3.1	16.4	0.1
95HE	1.5	2.4	19.6	3.3
90HE	1.8	2.8	24.1	7.8

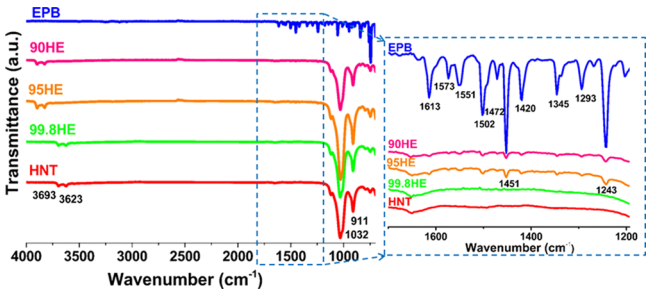

Figure 3. ATR-FTIR spectra of HNTs and HNTs modified with EPB.

defects, tends to be electrophilic due the presence of metal atoms, such as Al, consider a Lewis acid (an electron pair acceptor).[36] Thus, the HNT surface is favorable to interact with EPB, which has a conjugated structure and electron donor groups, such as N and O. Repulsion between HNT tubes modified with EPB may occur due to electrostatic and steric interactions, improving the tubes' stabilization. The same effect was observed by Cavallaro et al. (2014) when the HNT was modified with sodium alkanoates.[37]

3.2. BET Specific Surface Area. The specific surface area of samples was determined according to the BET method. Pristine halloysite had a type II adsorption isotherm (see the Supporting Information). This type of isotherm exhibits a flat behavior in regions of low relative pressure (P/Po < 0.8) and tends to increase rapidly in regions of high relative pressure (P/Po > 0.8). HNTs have a specific surface area of 54 m^2/g (Table 3) close to that reported in the literature.[4,18] The *C* constant in the BET method reflects the interaction between nitrogen gas molecules and the HNT surface. The higher the C value, the greater the energy interaction between the gas N_2 and the HNT surface (Al–OH/Si–OH free groups). For the pristine HNT, this value was 155. The specific surface area tends to decrease with an increase in the amount of EPB, as well as *C* constant. The decrease in specific surface area could be because EPB can occupy the HNT lumen space, reducing the total surface area of the tube. The hydroxyls on the HNT surface may have formed a hydrogen bond with the N and O of EPB and therefore be less available to interact with the nitrogen gas of the analysis, which would explain the reduction in the *C* constant. The same trend of results was observed by other authors upon HNT functionalization.[10,22]

Particle size of samples was also calculated using the BET surface area. After modification, the observed increase in particle size agrees with the DLS results. However, the particle size determined by the BET method was smaller than the size obtained by DLS, which could be related to greater tube agglomeration in DLS analysis.

3.3. Hydrophobicity Experiment. The results of water/toluene affinity tests are provided in Figure 2. The pristine HNT due to its more hydrophilic character stayed in the water phase but did not undergo swelling. The functionalized HNT underwent a partial migration to the toluene phase, which can be attributed to a more organophilic character obtained by modification of HNT with EPB. As explained before, the EPB and HNT bond is attributed to multiple mechanisms, which are considered weaker interactions than covalent bonds. The fact that EPB is not a typical surfactant or macromolecule could explain why part of the HNT remains in water after 24 h. This is different from what was observed in functionalization with a cationic surfactant, as reported by Cavallaro et al. (2015).[6]

3.4. Tensiometry. In tensiometry, the *n*-hexane was used to perform the calibration curve and determine the *C* constant for each sample. After determining the *C* constant, the modified Washburn equation (eq 2) was used to calculate the contact angle of each sample in three solvents (water, ethanol, and ethylene glycol) with different characteristics (Table 1), as explained before. The contact angle values were used to determine the surface energy of both pristine and modified HNT powders according to the Owens–Wendt–Kaelble method. The linearization curves were utilized to calculate these surface energies (see the Supporting Information). According to tensiometry results shown in Table 4, the pristine HNT has a surface energy of 29 mN/m decomposed into polar and dispersive components, whose values are 28 and 1.7mN/m, respectively. The polar (more hydrophilic character) component was higher than the dispersive (more hydrophobic character) one, which corroborates the hydrophobicity experiment, again affirming a more hydrophilic character of the HNT. The presence of EPB may affect the intermolecular interaction (cohesion) of molecules; thus, after HNT functionalization, the total surface energy of the system reduced and was accompanied by polar component reduction, revealing that the modified HNT tends to be more hydrophobic than the pristine one. This may indicate that EPB is an interesting candidate to be used as a coupling agent in HNT polymeric composites. A small difference in the surface energy levels between the polymer and filler is responsible for improving the interfacial interaction, allowing the polymer to be wet by the polymeric matrix, which affects

https://dx.doi.org/10.1021/acsanm.0c02600
ACS Appl. Nano Mater. 2020, 3, 11510–11516

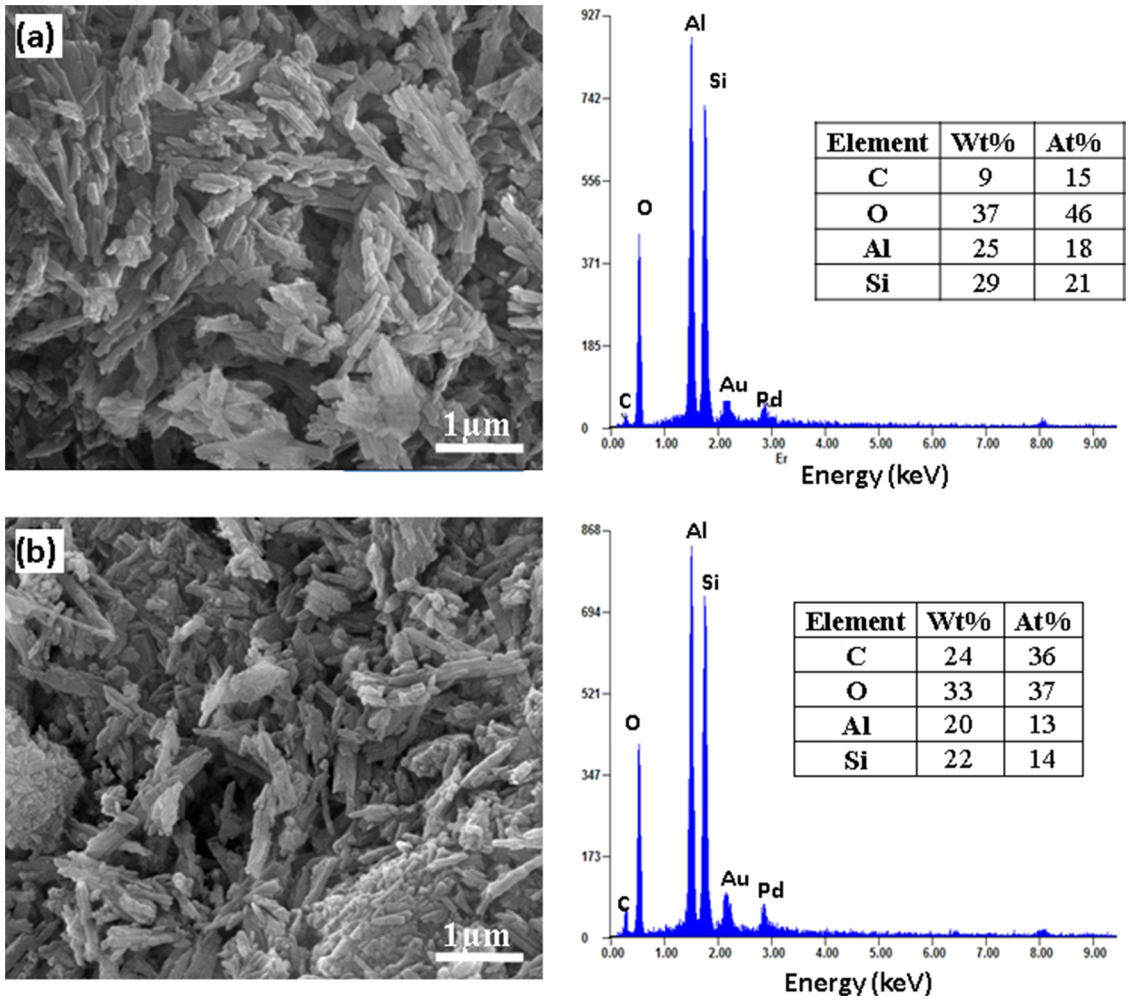

Figure 4. SEM image with 50X magnification and EDS of (a) pristine HNT and (b) HNT modified with EPB.

the stress transfer from the matrix to the filler at their interfaces.[38]

The samples of 99.8HE present curves with different angular coefficients when ethylene glycol was used, which does not guarantee certainty in the contact angles of 99.8HE with this solvent. This may be related to a lower homogeneity of the sample due to a reduced amount of EPB (0.2 wt %) in relation to the other samples.

3.5. Thermogravimetric Analysis. Thermogravimetric results for pure and modified HNTs are presented in Table 5 (see the curves in the Supporting Information), respectively. The mass loss in the range of temperature between 25 and 100 °C is related to the release of physically adsorbed water. The pristine HNT presented the highest mass loss. Samples functionalized with EPB exhibited a decrease in the mass loss in this range of temperature, indicating that modification was responsible for lowering the surface affinity for free water adsorption. In the second range of temperature (100−250 °C), HNT interlamellar water loss occurred. HNTs also had a greater mass loss than functionalized nanotubes, indicating a reduction in interlamellar water with functionalization. In the range of temperature between 250 and 650 °C, functionalized samples presented a greater mass loss than the pristine halloysite, indicating the degradation of EPB. Similar tendencies were observed by Pontón et al. (2014) for modified titanate nanotubes.[39] At the higher temperature range (250−650 °C), the EPB wt % concentration could be estimated, that is, for 99.8HE 0.1%, for 95HE 3.3%, and for 90HE 7.8%. The values were close to the EPB theoretical concentrations used.

3.6. Attenuated Total Reflection−Fourier Transform Infrared Spectroscopy. ATR-FTIR spectra of HNTs present characteristic bands (Figure 3) at 3693 and 3623 cm^{-1} related to OH stretching vibrations, at 1032 cm^{-1} related to Si−O (Si−O−Si and O−Si−O) stretching vibrations, and 911 cm^{-1} related to OH deformation vibrations.[5,16,21,40,41] In samples of HNT functionalized with EPB, bands related to aromatic C═C bonds appear between 1600 and 1400 cm^{-1} and bands related to aromatic C−N appear between 1340 and 1250 cm^{-1}, which are characteristic of EPB.[42]

3.7. SEM Analysis. The SEM images and EDS spectra of pristine and modified halloysite are presented in Figure 4a and b, respectively. SEM images display a typical acicular morphology with some agglomerates for both samples. The EDS spectra indicate the presence of Si, Al, and O elements for both samples; these elements are expected for aluminum silicate clay. The presence of the C element in pristine halloysite is due to the carbon tape used to deposit the sample in the holder. The C content increased in the sample modified with EPB, which may be due to the presence of carbon in the EPB structure.

https://dx.doi.org/10.1021/acsanm.0c02600
ACS Appl. Nano Mater. 2020, 3, 11510−11516

4. CONCLUSIONS

According to the literature, the electron deficiency of HNTs allows it to accept foreign electrons on its empty orbital, so when HNTs are blended with electron-rich species, electron transferring to HNTs can occur. In the present study, the organic conjugated structure of EPB was studied as an electron-rich species to modified halloysite. Increasing the amount of EPB, the interaction between it and the HNT became more evident. The chemical and physical properties determined by a set of characterization techniques together evidence this modification. The interactions between the halloysite and EPB may involve multiple mechanisms, such as Lewis acid−base, van der Waals forces, and electron transfer that can explain these results. The inner and edge surfaces of HNTs, sometimes even its surface defects, tend to be electrophilic due to the presence of metal atoms, such as Al, consider a Lewis acid (an electron pair acceptor). Therefore, the HNT surface is favorable to interact with EPB, which has a conjugated structure and electron donor groups, such as N and O. EPB could be a possible coupling agent for incorporation of modified halloysite in a polymeric matrix.

■ ASSOCIATED CONTENT

Supporting Information

The Supporting Information is available free of charge at https://pubs.acs.org/doi/10.1021/acsanm.0c02600.

BET adsorption isotherm curve; tensiometry linearization curves to calculate the surface energies; and thermogravimetric curves for pure HNTs and HNTs modified with EPB (PDF).

■ AUTHOR INFORMATION

Corresponding Author

Danae L. Francisco − *Group for Bionanomanufacturing (BIONANO), Laboratory of Chemical Process and Particle Technology (LPP), Institute for Technological Research of State of São Paulo (IPT), 05508-901 São Paulo, Brazil; Center for Chemical and Environmental Technology (CQMA), Nuclear and Energy Research Institute (IPEN), 05508-000 São Paulo, Brazil;* orcid.org/0000-0002-3297-5684; Email: danae_lopes@hotmail.com

Authors

Lucilene B. Paiva − *Group for Bionanomanufacturing (BIONANO), Laboratory of Chemical Process and Particle Technology (LPP), Institute for Technological Research of State of São Paulo (IPT), 05508-901 São Paulo, Brazil;* orcid.org/0000-0003-3047-7005

Wagner Aldeia − *Group for Bionanomanufacturing (BIONANO), Laboratory of Chemical Process and Particle Technology (LPP), Institute for Technological Research of State of São Paulo (IPT), 05508-901 São Paulo, Brazil*

Ademar B. Lugão − *Center for Chemical and Environmental Technology (CQMA), Nuclear and Energy Research Institute (IPEN), 05508-000 São Paulo, Brazil*

Esperidiana A. B. Moura − *Center for Chemical and Environmental Technology (CQMA), Nuclear and Energy Research Institute (IPEN), 05508-000 São Paulo, Brazil*

Complete contact information is available at: https://pubs.acs.org/10.1021/acsanm.0c02600

Author Contributions

All authors have approved the final version of the manuscript.

Notes

The authors declare no competing financial interest.

■ ACKNOWLEDGMENTS

The authors thank the Nuclear and Energy Research Institute (IPEN), the Institute for Technological Research of the State of São Paulo (IPT), FAPESP (Process Number 2019/00862-9), the National System of Nanotechnology Laboratories (SisNANO), and CNPq (Process Number: 402298/2013-6) for financial support.

■ ABBREVIATIONS

APTES, γ-aminopropyltriethoxysilane or 3-aminopropyltriethoxysilane;
AEAPTMS, *N*-2-aminoethyl-3-aminopropyltrimethoxysilane;
BrTMS, (3-bromopropyl)-trimethoxysilane;
BBT, 2,5-bis(2-benzoxazolyl) thiophene;
CNTs, carbon nanotubes;
EPB, (2,2′-(1,2-ethenediyldi-4,1-phenylene)-bisbenzoxazole);
GMA, glycidyl methacrylate;
GPS, γ-glycidoxypropyltrimethoxy;
MAPTS, γ-methacryloxypropyltrimethoxysilane or 3-(trimethoxysilyl)propyl methacrylate;
MPTMS, (3-mercaptopropyl)trimethoxysilane;
PhTES, phenyltriethoxysilane;
PPA, phenylphosphonic acid;
VTMS, vinyltrimethoxysilane;
TEM, transmission electron microscopy;
SEM, scanning electron microscopy;
EDS, energy-dispersive X-ray spectroscopy;
DRIFT, diffuse reflectance infrared Fourier transform;
DLS, dynamic light scattering;
DE, deuteration experiment;
BET, Brunauer−Emmett−Teller;
XRD, X-ray diffraction;
BJH, Barrett−Joyner−Halenda;
EA, elemental analysis;
XPS, X-ray photoelectron spectroscopy;
TG, thermogravimetry analysis;
ATR-FTIR, attenuated total reflectance− Fourier transform infrared;
NMR, nuclear magnetic resonance;
AFM, atomic force microscopy;
DSC, differential scanning calorimetry;
Py-GC/MS, pyrolysis−gas chromatography/mass spectrometry.

■ REFERENCES

(1) Liu, M.; Jia, Z.; Jia, D.; Zhou, C. Recent Advance in Research on Halloysite Nanotubes-Polymer Nanocomposite. *Prog. Polym. Sci.* **2014**, *39*, 1498−1525.
(2) Yuan, P.; Bergaya, F.; Thill, A. *General Introduction*, 1st ed.; Elsevier Ltd., 2016; 7. DOI: 10.1016/B978-0-08-100293-3.00001-7.
(3) Tan, D.; Yuan, P.; Liu, D.; Du, P. Surface Modifications of Halloysite. *Develop. in Clay Sci.* **2016**, *7*, 167−201.
(4) Liu, M.; Guo, B.; Du, M.; Cai, X.; Jia, D. Properties of Halloysite Nanotube-Epoxy Resin Hybrids and the Interfacial Reactions in the Systems. *Nanotechnology* **2007**, *18*, 455703.

(5) Szpilska, K.; Czaja, K.; Kudla, S. Halloysite Nanotubes as Polyolefin Fillers. *Polimery/Polymers* **2015**, *60*, 359−371.
(6) Cavallaro, G.; Lazzara, G.; Milioto, S.; Parisi, F. Hydrophobically Modified Halloysite Nanotubes as Reverse Micelles for Water-in-Oil Emulsion. *Langmuir* **2015**, *31*, 7472−7478.
(7) Yang, H.; Zhang, Y.; Ouyang, J. Physicochemical Properties of Halloysite, 1st ed.; Elsevier Ltd., 2016; 7. DOI: 10.1016/B978-0-08-100293-3.00004-2.
(8) Yuan, P.; Tan, D.; Annabi-Bergaya, F. Properties and Applications of Halloysite Nanotubes: Recent Research Advances and Future Prospects. *Appl. Clay Sci.* **2015**, *112-113*, 75−93.
(9) Yang, Y.; Chen, Y.; Leng, F.; Huang, L.; Wang, Z.; Tian, W. Recent Advances on Surface Modification of Halloysite Nanotubes for Multifunctional Applications. *Appl. Sci.* **2017**, *7*, 1215.
(10) Peixoto, A. F.; Fernandes, A. C.; Pereira, C.; Pires, J.; Freire, C. Physicochemical Characterization of Organosilylated Halloysite Clay Nanotubes. *Microporous Mesoporous Mater.* **2016**, *219*, 145−154.
(11) Yuan, P.; Southon, P. D.; Liu, Z.; Green, M. E. R.; Hook, J. M.; Antill, S. J.; Kepert, C. J. Functionalization of Halloysite Clay Nanotubes by Grafting with γ -Aminopropyltriethoxysilane. *RSC* **2008**, *7*, 15742−24148.
(12) Yuan, P.; Tan, D.; Aannabi-Bergaya, F.; Yan, W.; Fan, M.; Liu, D.; He, H. Changes in Structure, Morphology, Porosity, and Surface Activity Of Mesoporous Halloysite Nanotubes Under Heating. *Clays Clay Miner.* **2012**, *60*, 561−573.
(13) Zeng, G.; He, Y.; Zhan, Y.; Zhang, L.; Shi, H.; Yu, Z. Preparation of a Novel Poly(Vinylidene Fluoride) Ultrafiltration Membrane by Incorporation of 3-Aminopropyltriethoxysilane-Grafted Halloysite Nanotubes for Oil/Water Separation. *Ind. Eng. Chem. Res.* **2016**, *55*, 1760−1767.
(14) Erdogan, A. R.; Kaygusuz, I.; Kayanak, C. Influences of Aminosilanization of Halloysite Nanotubes on the Mechanical Properties of Polyamide-6 Nanocomposites. *Polym. Compos.* **2014**, *35*, 1350−1361.
(15) Sahnoune, M.; Taguet, A.; Otazaghine, B.; Kaci, M.; Lopez-Cuesta, J. M. Effects of Functionalized Halloysite on Morphology and Properties of Polyamide-11/SEBS-g-MA Blends. *Eur. Polym. J.* **2016**, *90*, 418−430.
(16) Krishnaiah, P.; Ratnam, C. T.; Manickam, S. Development of Silane Grafted Halloysite Nanotube Reinforced Polylactide Nanocomposites for the Enhancement of Mechanical, Thermal and Dynamic-Mechanical Properties. *Appl. Clay Sci.* **2017**, *135*, 583−595.
(17) Albdiry, M. T.; Yousif, B. F. Morphological Structures and Tribological Performance of Unsaturated Polyester Based Untreated/Silane-Treated Halloysite Nanotubes. *Mater. Des.* **2013**, *48*, 68−76.
(18) Pasbakhsh, P.; How, H. K.; Piao, C. S. *Modification of Halloysite Nanotubes with Glycidyl Methacrylate Samples of Jarrahdale Obtained from a Laterite Pallid Zone near Jarrahdale, 50 Km Southeast Of*. 2012, 1−4.
(19) Taroni, T.; Meroni, D.; Fidecka, K.; Maggioni, D.; Longhi, M.; Ardizzone, S. Halloysite Nanotubes Functionalization with Phosphonic Acids: Role of Surface Charge on Molecule Localization and Reversibility. *Appl. Surf. Sci.* **2018**, *486*, 466−473.
(20) Guo, B.; Zou, Q.; Lei, Y.; Jia, D. Structure and Performance of Polyamide 6/Halloysite Nanotubes Nanocomposites. *Polym. J.* **2009**, *41*, 835−842.
(21) Pasbakhsh, P.; Ismail, H.; Fauzi, M. N. A.; Bakar, A. A. EPDM/Modified Halloysite Nanocomposites. *Appl. Clay Sci.* **2010**, *48*, 405−413.
(22) Liu, M.; Guo, B.; Du, M.; Lei, Y.; Jia, D. Natural Inorganic Nanotubes Reinforced Epoxy Resin Nanocomposites. *J. Polym. Res.* **2008**, *15*, 205−212.
(23) Liu, M.; Guo, B.; Du, M.; Jia, D. The Role of Interactions between Halloysite Nanotubes and 2,2′-(1,2-Ethenediyldi-4,1-Phenylene) Bisbenzoxazole in Halloysite Reinforced Polypropylene Composites. *Polym. J.* **2008**, *40*, 1087−1093.
(24) Liu, M.; Guo, B.; Zou, Q.; Du, M.; Jia, D. Interactions between Halloysite Nanotubes and 2,5-Bis(2-Benzoxazolyl) Thiophene and Their Effects on Reinforcement of Polypropylene/Halloysite Nanocomposites. *Nanotechnology* **2008**, *19*, 205709.
(25) Marney, D. C. O.; Yang, W.; Russell, L. J.; Shen, S. Z.; Nguyen, T.; Yuan, Q.; Varley, R.; Li, S. Phosphorus Intercalation of Halloysite Nanotubes for Enhanced Fire Properties of Polyamide 6. *Polym. Adv. Technol.* **2012**, *23*, 1564−1571.
(26) Cavallaro, G.; Grillo, I.; Gradzielski, M.; Lazzara, G. Structure of Hybrid Materials Based on Halloysite Nanotubes Filled with Anionic Surfactants. *J. Phys. Chem. C* **2016**, *120*, 13492−13502.
(27) Ghoroi, C.; Shukla, P.; Karde, V.; Thakker, M.; Shah, D. O. Wettability Measurement Apparatus for Porous Material Using the Modified Washburn Method. *Meas. Sci. Technol.* **2013**, *24*, 125902.
(28) Heertjes, P. M.; Kossen, N. W. F. Measuring the Contact Angles of Powder-Liquid Systems. *Powder Technol.* **1967**, *1*, 33−42.
(29) Bartell, F. E.; Whitney, C. E. Adhesion Tension a Receding Contact Angle, Pressure of Displacement Method. *J. Phys. Chem.* **1932**, *36*, 3115−3126.
(30) Washburn, E. W. Note on the Dynamics of Capillary Flow. *Phys. Rev.* **1921**, *18*, 206−209.
(31) Wohlleben, W.; Mielke, J.; Bianchin, A.; Ghanem, A.; Freiberger, H.; Rauscher, H.; Gemeinert, M.; Hodoroaba, V. D. Reliable Nanomaterial Classification of Powders Using the Volume-Specific Surface Area Method. *J. Nanopart. Res.* **2017**, *19*, 61.
(32) Lecloux, A. J.; Atluri, R.; Kolen'ko, Y. V.; Deepak, F. L. Discussion about the Use of the Volume Specific Surface Area (VSSA) as a Criterion to Identify Nanomaterials According to the EU Definition. Part Two: Experimental Approach. *Nanoscale* **2017**, *9*, 14952−14966.
(33) Pan, Q.; Li, N.; Hong, Y.; Tang, H.; Zheng, Z.; Weng, S.; Zheng, Y.; Huang, L. Halloysite Clay Nanotubes as Effective Nanocarriers for the Adsorption and Loading of Vancomycin for Sustained Release. *RSC Adv.* **2017**, *7*, 21352−21359.
(34) Veerabadran, N. G.; Price, R. R.; Lvov, Y. M. Clay Nanotubes for Encapsulation and Sustained Release of Drugs. *NANO* **2007**, *02*, 115−120.
(35) Huang, J.; Tang, Z. H.; Zhang, X. H.; Guo, B. C. *Halloysite Polymer Nanocomposites*, 1st ed.; Elsevier Ltd., 2016; 7. DOI: 10.1016/B978-0-08-100293-3.00021-2.
(36) Saif, M. J.; Asif, H. M.; Naveed, M. Properties and Modification Methods of Halloysite Nanotubes: A State-of-The-Art Review. *J. Chil. Chem. Soc.* **2018**, *63*, 4109−4125.
(37) Cavallaro, G.; Lazzara, G.; Milioto, S.; Parisi, F.; Sanzillo, V. Modified Halloysite Nanotubes: Nanoarchitectures for Enhancing the Capture of Oils from Vapor and Liquid Phases. *ACS Appl. Mater. Interfaces* **2014**, *6*, 606−612.
(38) Li, Y.; Huang, Y.; Krentz, T.; Natarajan, B.; Neely, T.; Schadler, L. S. Interface/Interphase *in Polymer Nanocomposites*; Netravali, A. N., Mittal, K. L., Eds.; John Wiley & Sons, Inc.: Hoboken, NJ, USA, 2016. DOI: 10.1002/9781119185093.
(39) Pontón, P. I.; D'Almeida, J. R. M.; Marinkovic, B. A.; Savić, S. M.; Mancic, L.; Rey, N. A.; Morgado, E.; Rizzo, F. C. The Effects of the Chemical Composition of Titanate Nanotubes and Solvent Type on 3-Aminopropyltriethoxysilane Grafting Efficiency. *Appl. Surf. Sci.* **2014**, *301*, 315−322.
(40) Saikia, B. J.; Parthasarathy, G. Fourier Transform Infrared Spectroscopic Characterization of Kaolinite from Assam and Meghalaya, Northeastern India. *J. Mod. Phys.* **2010**, *01*, 206−210.
(41) Kumanayaka, T. O.; Parthasarathy, R.; Jollands, M. Accelerating Effect of Montmorillonite on Oxidative Degradation of Polyethylene Nanocomposites. *Polym. Degrad. Stab.* **2010**, *95*, 672−676.
(42) Coates, J. Encyclopedia of Analytical Chemistry-IInterpretation of Infrared Spectra, A Practical Approach. *Encycl. Anal. Chem.* **2004**, 1−23.